

OCCURRENCE OF *LREE*- AND Y-ARSENATES FROM A Fe–Mn DEPOSIT, LIGURIAN BRIANÇONNAIS DOMAIN, MARITIME ALPS, ITALY

ROBERTO CABELLA[§], GABRIELLA LUCCHETTI AND PIETRO MARESCOTTI

Dipartimento per lo Studio del Territorio e delle Sue Risorse, Università di Genova, C.so Europa, 26, I-16132 Genova, Italy

ABSTRACT

We report the occurrence of some rare and unknown *LREE*- and Y-arsenates. They are present within the Ponte dei Gorrazzi Fe–Mn deposit, associated with quartz arenites and subordinately with marbles of the Corsaglia Valley sequence, in the Ligurian Briançonnais Domain, Maritime Alps, Italy. These minerals mainly occur within microveins and microcavities as microcrystalline aggregates or small isolated prismatic crystals (up to 10 μm in length). Three different groups have been distinguished on the basis of electron-microprobe data. 1) Group A is characterized by Y-rich grains with low *LREE* contents whose composition is consistent with the formula of chernovite (YAsO_4). 2) Group B is characterized by *LREE*-rich grains (mainly La), with very low Y contents; their chemical composition does not correspond to any known natural phase, but it is consistent with that of the synthetic compound LaAsO_4 . 3) Group-C grains are characterized by intermediate contents of Y and the *LREE*. Although they could be related to micrometer-scale intergrowths of Group A and B minerals, they are characterized by significant enrichments in Gd, Th and Ca, thus suggesting the possibility of a distinct mineral species.

Keywords: arsenates, chernovite, mineral chemistry, Fe–Mn deposit, Maritime Alps, Italy.

SOMMAIRE

Nous décrivons ici la présence d'arsénates rares et inconnus, enrichis en terres rares légères et en yttrium. Ils ont été découverts dans le minerai du gisement de Fe–Mn de Ponte dei Gorrazzi, associé aux arénites quartzifères et, de façon plus aléatoire, aux marbres de la séquence de la vallée de Corsaglia, dans le domaine ligurien briançonnais, Alpes Maritimes, en Italie. Ces minéraux tapissent les parois de microveines et de microcavités sous forme d'aggrégats microcristallins ou de petits cristaux prismatiques isolés atteignant une longueur de 10 μm . Nous distinguons trois groupes, selon les données sur la composition obtenues avec une microsonde électronique. 1) Les grains du groupe A montrent un enrichissement en yttrium, et ont une faible teneur en terres rares légères; leur composition concorde avec la stoechiométrie de la chernovite (YAsO_4). 2) Les grains du groupe B montrent un enrichissement en terres rares légères, surtout le La, avec une teneur très faible en yttrium. Leur composition ne correspond pas à celle d'un minéral connu, mais plutôt à celle du composé synthétique LaAsO_4 . 3) Les grains du groupe C se distinguent par une composition intermédiaire en termes de leur teneur en Y et en terres rares légères. Quoique ceux-ci pourraient bien représenter une intercroissance micrométrique de minéraux des groupes A et B, ils ont aussi une teneur importante en Gd, Th et Ca, et pourraient donc être une espèce distincte.

(Traduit par la Rédaction)

Mots-clés: arsenates, chernovite, composition des minéraux, gisement de Fe–Mn, Alpes Maritimes, Italie.

INTRODUCTION

Y- and *LREE*-minerals are present as magmatic accessory phases, mainly in granites, carbonatites, pegmatites, alkaline and peralkaline igneous rocks (Chang *et al.* 1996, and references therein; Wyllie *et al.* 1996, Wu *et al.* 1996) and as secondary products related to the circulation of hydrothermal fluids (Gieré 1996). We have found chernovite-type (YAsO_4) and other unknown arsenates of the light rare-earths (*LREE*) in a small Fe–Mn deposit known as Ponte dei Gorrazzi, associated with quartz arenites and marbles of the

Corsaglia Valley sequence, exposed in the Maritime Alps, Italy. They mainly occur as scattered micrometric grains or cryptocrystalline aggregates in microveins and microcavities. In this paper, we report results of a systematic study of the mineral chemistry of these phases and propose a hypothesis for their formation.

GEOLOGICAL SETTING

The Corsaglia Valley sequence is located in the Internal Briançonnais Domain (Fig. 1a). This domain is characterized by a pre-Carboniferous crystalline

[§] E-mail address: cabella@dipteris.unige.it

basement and Permian calc-alkaline volcanic rocks (mainly rhyolites) overlain by Triassic to Eocene sedimentary sequences. The Corsaglia Valley sequence consists of sedimentary rocks varying in age from upper Permian to upper Cretaceous (Fig. 1b). These rocks are related to two cycles of subsidence and transgression, which occurred during the pre-rifting and rifting stages of the Ligurian–Piemontese Ocean. The beginning of these cycles is marked by early Triassic quartzites, the upper Jurassic conglomerates and quartz arenites, respectively (Vanossi *et al.* 1986, Dallagiovanna 1993). During the Alpine tectonometamorphic evolution, the whole sequence underwent polyphase metamorphism under blueschist-facies conditions ($P \geq 7$ kbars, $T = 300 \pm 50^\circ\text{C}$), followed by a decompression-induced retrograde evolution (Vanossi *et al.* 1986, Dallagiovanna 1993, and references therein). The Fe–Mn deposit is located near the base of upper Jurassic limestones of the Corsaglia Valley sequence, within quartz arenites and marbles horizons (Fig. 1b).

ANALYTICAL METHODS

The arsenate minerals have been identified in polished sections with a scanning electron microscope (SEM). Because of their paucity and the very small dimensions, it was not possible to separate the minerals for X-ray-diffraction (XRD) analysis, either through hand picking or with magnetic separation.

Qualitative chemical analyses were carried out in energy-dispersion mode (EDS) with a scanning electron microscope (SEM, Philips 515) equipped with an X-ray energy-dispersion analyzer (EDAX PV9100) using an accelerating voltage of 15 kV and a beam current of about 2 nA.

Quantitative analyses were performed with an ARL–SEM-Q electron microprobe in wavelength-dispersion mode (WDS) using an accelerating voltage of 20 kV (sample current of 20 nA) with a beam size of about 4 μm , peak and background counting times of 40 and 10 seconds, respectively. The reference standards *REE1*, *REE2*, *REE3* and *REE4* (Drake & Weill 1972), synthetic glasses (ThO_2 100%, Y_2O_3 100%), synthetic compounds (apatite, arsenolite, zirconia, NdSi, PrSi, Ce_2YSi_2 , La_2YSi_2 , metallic V), and natural phases (monazite, albite, “hortonolite”), were used as standards. The lines used for analysis, the interfering elements, and detection limits for each element are reported in Table 1. Interference effects due to peak overlaps were minimized using the PROBE 5.2 software (Donovan & Rivers 1990). The accuracy and precision of the analyses and the interference-correction effects at different levels of concentration were checked using the same analytical standards as unknowns during the analytical runs. The observed analytical error (E) varies strongly in each analysis depending on the concentration of an element (X): $X \geq 10\%$, $E \leq 1\%$; $1 \leq X \leq 10\%$, $E \leq 15\%$, and $X \leq 1\%$, $E > 15\%$.

TABLE 1. LINES USED FOR ELECTRON-MICROPROBE ANALYSIS, INTERFERING ELEMENTS, AND CALCULATED LIMITS OF DETECTION

element	line	crystal	limit of detection *	interfering elements °
As	La	RAP	0.01	Pr, Ce
V	K α	PET	0.01	Pr
P	K α	PET	0.01	
Si	K α	ADP	0.01	
Ca	K α	PET	0.01	
Y	La	ADP	0.04	
La	La	PET	0.03	
Ce	La	PET	0.03	
Pr	La	PET	0.03	V
Nd	La	LiF200	0.06	Ce
Sm	La	LiF200	0.05	Ce
Eu	La	LiF200	0.05	Pr, Nd
Gd	La	LiF200	0.05	Ce, La
Th	Ma	PET	0.03	

* Detection limits at 99% confidence in elemental weight % (Single Line).

° Interference corrections were made using the Probe 5.2 program (Donovan & Rivers 1990).

Bulk-rock analyses were carried out by X-ray fluorescence (XRF) on fused glass disks (major elements) and pressed powders (minor and trace elements) bound with a Mowiol solution; instrumentation consisted of a Philips PW1480 spectrometer with Rh and W tubes for major, some minor, and trace elements. Moreover, depending on the anomalously high contents of Mn, Fe, P, and As, suitable calibration curves have been used. Replicate analyses of rock standards show that the major-element data are precise to within 0.5% to 2.5%, and between 3% and 5% for Al, Na, and P. The trace-element data are considered accurate to between 2% and 3% or 1 ppm (whichever is greater) for Y, Rb, and Zr, and between 5% and 10% or 1 ppm for the others. The accuracy of the *LREE* in some cases was considerably lower.

Fe–Mn DEPOSIT OF THE CORSAGLIA VALLEY

The Ponte dei Gorrazzi deposit was mined for Fe in the 19th century. Fe–Mn ore occurs in quartz arenites as black massive recrystallized layers (up to 10 cm in thickness), lens-shaped decimetric boudins, and subordinately in «ptygmatic» mineralized veins; in the adjoining marbles, it occurs as thin recrystallized layers (up to 10 mm in thickness) and as subelliptical boudins (up to 2 cm in diameter). The Fe–Mn deposit and adjoining rocks contain widespread detrital constituents, mainly represented by polycrystalline rounded quartz pebbles (rarely exceeding 1 cm) and apatite grains. Grains of subhedral zircon (up to some mm in length) are occasionally concentrated in millimetric layers. Secondary hematite-bearing veinlets (up to tens of millimeters) cross-cut both quartz arenites and marbles.

Mineralized layers and lenses are characterized by cryptomelane-group minerals \pm hematite \pm braunite,

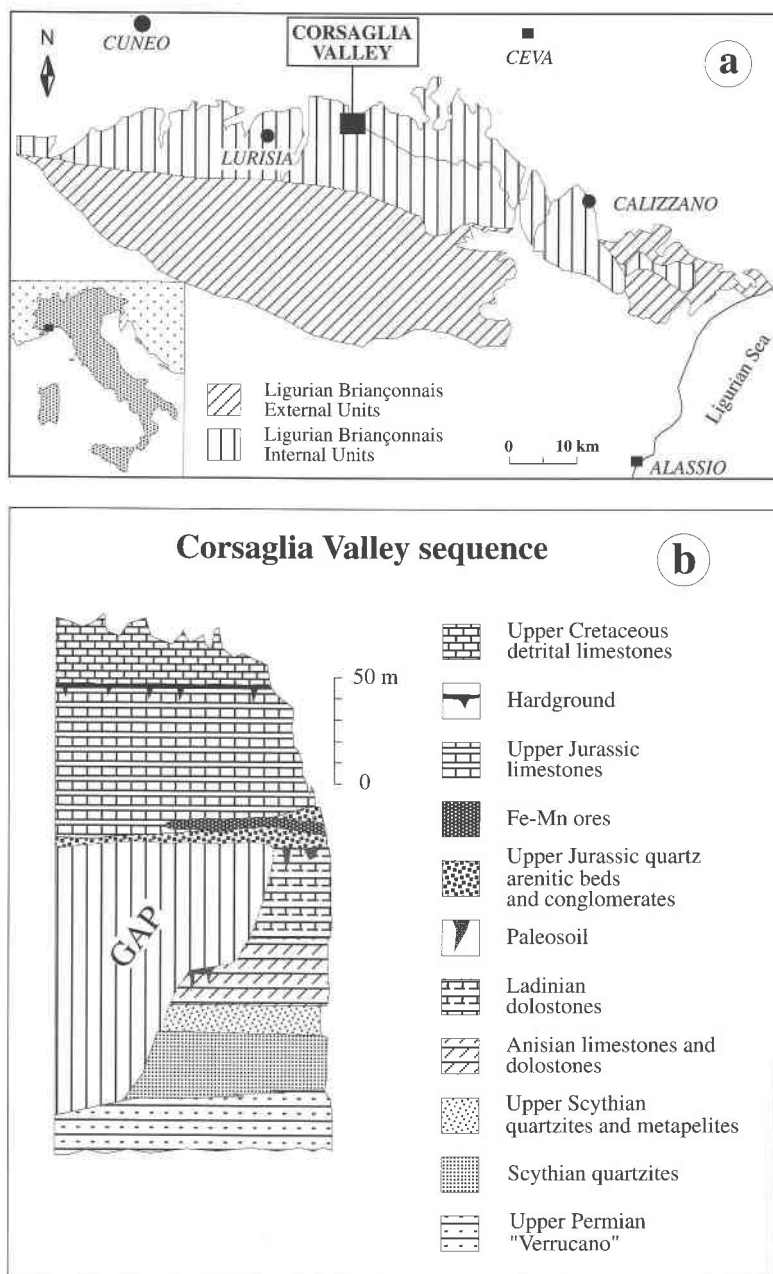


Fig. 1. a) Location map of the Corsaglia Valley sequence. b) Stratigraphic sequence of Corsaglia Valley (simplified from Cabella *et al.* 1995).

with variable amounts of quartz, calcite, Mn- and Fe-rich phengitic mica and aegirine; they represent the result of the metamorphic evolution of pristine sedimentary Fe-Mn-rich layers interbedded with siliciclastic and carbonate sediments (Cabella *et al.* 1992). Whole-rock chemical compositions (Table 2) reveal significant

differences between Fe-Mn ores and their host rocks; as shown in Figures 2a and b, heavy metals such as Ni, Co, Cu, Cr, Zn, and Pb, together with P, As, La, Nd, and Y, are clearly partitioned into the ores. It is not clear when this fractionation took place, but it probably reflects a primary feature that has not been significantly

modified during the metamorphic re-equilibration. In fact, as observed in many Fe–Mn ores of various types, these elements can be efficiently partitioned into the ores through scavenging processes by Fe and Mn oxyhydroxide particles and therefore, can be adsorbed in the primary ore minerals (Roy 1981, and references therein; Kunzendorf *et al.* 1993, Glasby *et al.* 1997).

The primary origin of Fe and Mn enrichments, however, is still doubtful because of the pervasive metamorphic overprint. Nevertheless, on the basis of geological and stratigraphic constraints, the deposition of Mn and Fe presumably took place in a shallow basin during the upper Jurassic transgression (Cabella *et al.* 1992).

As shown by Roy (1992), the source of Mn and Fe may be multiple, such as terrigenous input and distal

transport from hydrothermal vents along the active spreading centers of the neighboring Ligurian–Piemontese Ocean.

OCCURRENCE OF *LREE*- AND *Y*-ARSENATES

LREE- and *Y*-arsenates have been found mainly associated with the Fe–Mn ores. Their modal abundance drastically decreases from the mineralized layers and lenses toward the host rocks. At the scale of SEM observations, they appear brighter than the adjoining Mn- and Fe-oxides. Their shape varies from round to irregular to rarely prismatic and elongate.

The *LREE*- and *Y*-arsenates are present in three main modes of occurrence (Fig. 3a):

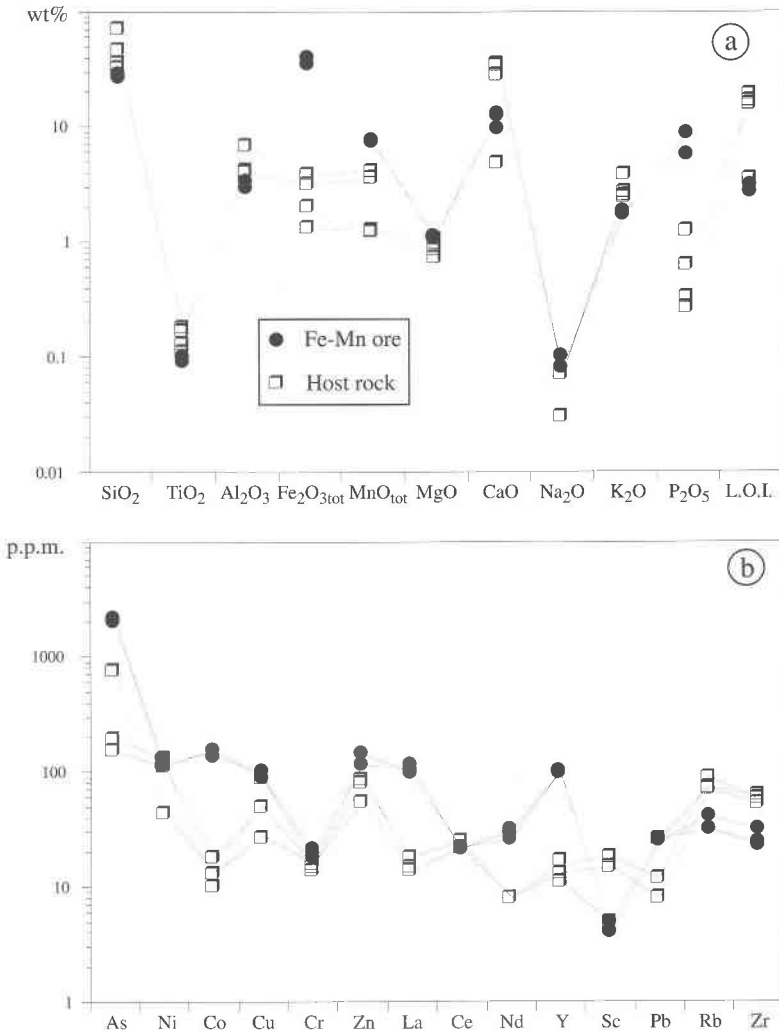


FIG. 2. Chemical composition of Fe–Mn ores and host-rocks: a) major elements, b) selected minor and trace elements.

1) Irregular lining or partial fillings of microveins: variable amounts of arsenates occur as aggregates of subhedral to anhedral crystals irregularly arranged within microveins, or subordinately along their walls (Fig. 3b). The microveins are irregularly distributed within the mineralized layers and lenses, where they cross-cut the granoblastic hematite \pm braunite \pm cryptomelane-group minerals \pm quartz assemblages. Most of the veins are characterized by sinuous to irregu-

lar shape, vary in width from some tens to 100 μm , and are filled by blocky aggregates of quartz together with phengitic mica and subordinate amounts of apatite \pm hematite \pm carbonates.

2) Partial or complete filling of intergranular microcavities: arsenates occur as anhedral or, rarely, prismatic elongate crystals (up to 10 μm in length) that line the walls of the cavities. In few exceptions, small rounded microcavities (up to 20 μm in diameter) are

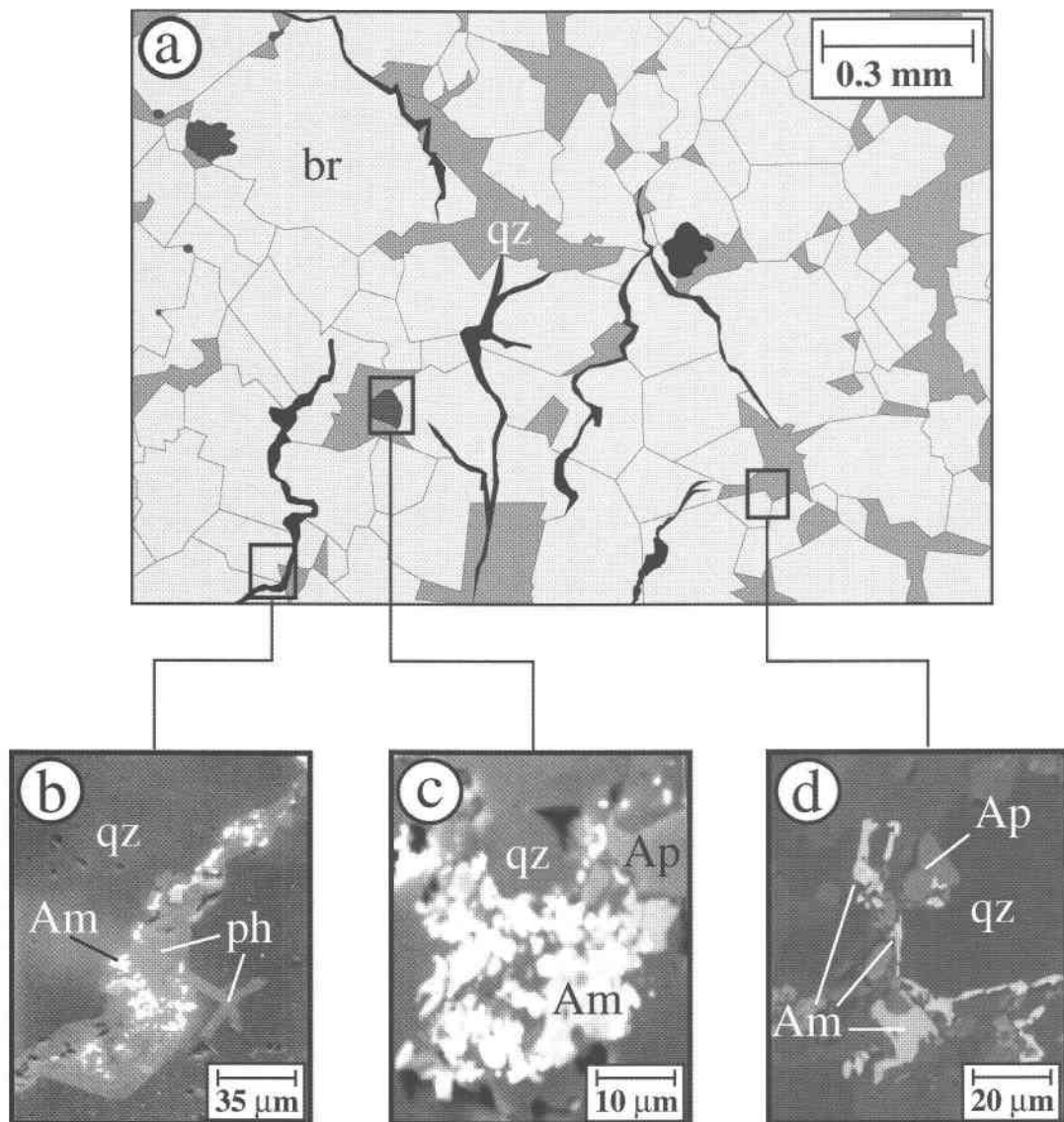


FIG. 3. Mode of occurrences of *LREE*- and *Y*-arsenates. a) Sketch of granoblastic ore assemblage drawn from reflected-light micrographs: light gray: braunite, medium gray: quartz, black: veins and cavities. Squares b), c), and d) show SEM micrographs of the three different modes of occurrence described in the text with the *LREE*- and *Y*-arsenates appearing as the lighter bright phases: b) microveins, c) microcavities, and d) lining of a quartz crystal. Abbreviations: Am: arsenate minerals, Ap: apatite, br: braunite, ph: phengite, qz: quartz.

TABLE 2. BULK-ROCK COMPOSITION OF Fe-Mn ORES AND HOST ROCKS, LIGURIAN BRIANÇONNAIS DOMAIN

	Fe-Mn ore			Host rock			D.L.
SiO ₂ wt%	27.19	26.80	28.77	46.68	70.65	35.61	0.03
TiO ₂	0.09	0.09	0.10	0.11	0.17	0.13	0.01
Al ₂ O ₃	2.95	2.97	3.40	4.12	6.83	4.29	0.01
Fe ₂ O ₃ tot	35.30	35.29	39.12	1.33	3.80	2.00	0.01
MnOtot	7.42	7.40	7.53	1.21	4.05	1.27	0.005
MgO	1.11	1.09	1.08	0.72	0.97	0.85	0.01
CaO	12.31	12.71	9.42	27.49	4.88	33.62	0.005
Na ₂ O	0.08	0.10	0.08	0.07	0.03	0.07	0.03
K ₂ O	1.69	1.74	1.78	2.48	3.83	2.71	0.01
P ₂ O ₅	8.58	8.49	5.66	0.27	1.24	0.32	0.01
L.O.I.	3.00	3.00	2.69	15.45	3.45	19.05	0.01
Total	99.72	99.68	99.63	99.93	99.90	99.92	
As ppm	2040	2015	2170	155	770	192	3
Ni	114	113	133	110	43	131	2
Co	154	156	134	18	13	9	2
Cu	89	90	101	49	27	88	2
Cr	19	18	21	16	16	15	5
Zn	117	116	146	54	85	81	2
La	106	117	98	14	15	18	5
Ce	21	21	22	22	< 5	25	5
Nd	31	29	26	8	< 5	8	5
Y	97	98	102	13	11	16	2
Sc	5	5	< 5	15	5	18	5
Pb	26	26	25	8	26	12	2
Rb	31	31	41	70	74	89	4
Zr	23	24	31	52	62	58	3

Analytical errors as discussed in the section on Analytical methods. D.L.: detection limits.

completely filled by aggregates of arsenates (Fig. 3c). The microcavities (from tens up to some hundreds of μm across) are subrounded or irregular, and are mainly located at the boundaries between Fe- and Mn-oxides and quartz. They are partially to completely filled with a mineral assemblage that is identical to the one observed in the veins.

3) Partial lining of braunite or quartz crystals (or both): trails of rod-shaped arsenate grains (up to some μm in length; Fig. 3d) line quartz and, subordinately, braunite crystals in granoblastic quartz + braunite \pm cryptomelane assemblages.

MINERAL CHEMISTRY

The analyzed minerals are arsenates, invariably consistent with the general formula $X\text{AsO}_4$ (X : *LREE*, Y, Ca, Th, Gd; Tables 3–5). Three distinct compositional groups, hereafter named Groups A–C, have been distinguished on the basis of the dominant X cation (Fig. 4). There is no evidence of correlations between the chemical compositions and the different mode of occurrence described above.

Group A is characterized by Y-rich, *LREE*-poor arsenates ($\text{Y}_2\text{O}_3 > 35 \text{ wt}\%$; $\text{LREE}_2\text{O}_3 < 13 \text{ wt}\%$; Table 3), whose composition is consistent with chernovite (YAsO_4). The major chemical variations are related to the substitution of *LREE* (up to 0.16 atoms per formula unit, *apfu*) for Y (Fig. 5a). The *LREE* are mainly

TABLE 3. ELECTRON-MICROPROBE DATA, GRAINS OF GROUP-A ARSENATE

	47.89	49.98	48.81	47.85	45.90	47.92	42.92	36.75
As ₂ O ₃ wt%	47.89	49.98	48.81	47.85	45.90	47.92	42.92	36.75
Y ₂ O ₃	1.70	< 0.02	< 0.02	0.83	0.24	1.12	0.35	0.54
P ₂ O ₅	0.13	0.09	0.09	0.09	3.21	0.18	4.13	9.17
SiO ₂	< 0.02	< 0.02	< 0.02	< 0.02	0.40	< 0.02	0.23	0.36
La ₂ O ₃	< 0.04	< 0.04	< 0.04	< 0.04	< 0.04	< 0.04	< 0.04	< 0.04
Ce ₂ O ₃	0.51	0.14	2.06	5.20	0.58	4.37	0.42	0.52
Pr ₂ O ₃	0.15	0.07	< 0.04	< 0.04	< 0.04	< 0.04	< 0.04	< 0.04
Nd ₂ O ₃	2.40	3.49	4.21	3.94	0.22	5.77	1.87	0.46
Sm ₂ O ₃	0.16	1.49	1.41	1.65	0.39	< 0.06	0.82	0.64
Eu ₂ O ₃	< 0.06	< 0.06	< 0.06	< 0.06	< 0.06	< 0.06	< 0.06	< 0.06
Gd ₂ O ₃	0.16	1.49	1.41	1.65	1.60	0.92	1.93	1.98
Y ₂ O ₃	46.72	42.75	41.35	36.34	46.90	39.10	35.45	46.11
ThO ₂	< 0.03	0.12	0.23	1.15	0.23	0.34	9.70	2.76
CaO	0.12	0.17	0.10	0.51	0.07	0.04	1.99	0.54
$\Sigma\text{LREE}_2\text{O}_3$	3.22	5.19	7.68	10.79	1.19	10.14	3.11	1.62
Total	99.94	99.79	99.67	99.21	99.74	99.76	99.81	99.83
Number of ions on the basis of 4 atoms of oxygen								
As <i>apfu</i>	0.955	1.011	1.001	0.993	0.897	0.980	0.869	0.702
V	0.043	-	-	0.022	0.006	0.029	0.009	0.013
P	0.004	0.003	0.003	0.003	0.102	0.006	0.135	0.283
Si	-	-	-	-	0.015	-	0.009	0.013
Total	1.002	1.014	1.004	1.018	1.020	1.015	1.022	1.011
La	-	-	-	-	-	-	-	-
Ce	0.007	0.002	0.030	0.076	0.008	0.063	0.006	0.007
Pr	0.002	0.001	-	-	-	-	-	-
Nd	0.033	0.048	0.059	0.056	0.003	0.081	0.026	0.006
Sm	0.002	0.020	0.019	0.023	0.005	-	0.011	0.008
Eu	-	-	-	-	-	-	-	-
Gd	0.002	0.019	0.018	0.022	0.020	0.012	0.025	0.024
Y	0.948	0.880	0.863	0.767	0.933	0.814	0.730	0.896
Ca	0.005	0.007	0.004	0.022	0.003	0.002	0.083	0.021
Th	-	0.001	0.002	0.010	0.002	0.003	0.085	0.023
ΣLREE	0.044	0.071	0.108	0.155	0.016	0.144	0.043	0.021
Total	0.999	0.978	0.995	0.976	0.974	0.975	0.966	0.985

Analytical errors as discussed in the section on Analytical methods.

represented by Ce (up to 0.08 *apfu*; Fig. 5b), Nd (up to 0.08 *apfu*; Fig. 5c), and Sm (up to 0.03 *apfu*; Fig. 5d). La, Pr, Eu and the heavy rare-earth elements (*HREE*), with the exception Gd (up to 0.03 *apfu*), are generally below the limits of detection. Th and Ca contents (Fig. 6) are generally low (< 0.02 *apfu*), although a few exceptions are noted. Arsenic can be replaced by P (up to 0.28 *apfu*) and subordinately by V (up to 0.05 *apfu*) (Figs. 7a–c).

Group B is characterized by *LREE*-rich (mainly La), Y-poor arsenates ($\text{Y}_2\text{O}_3 < 2 \text{ wt}\%$; $\text{LREE}_2\text{O}_3 > 53 \text{ wt}\%$; Table 4) whose composition is consistent with the formula LaAsO_4 . The major chemical variations are related to the replacement of La by other *LREE* (mainly Nd, Pr, and Ce) (Fig. 8a). The Ce, Nd and Pr contents are generally lower than 0.2 *apfu* (Figs. 8b–d), whereas Eu and Sm contents are generally below or near the limits of detection. A significant exception is represented by a Nd-dominant composition that approaches the formula NdAsO_4 (Fig. 8c, Table 4). The other chemical features are: a) wide range of V-for-As substitution (V up to 0.3 *apfu*; Fig. 7c) and, to a lesser extent, of P-for-As substitution ($\text{P} < 0.15 \text{ apfu}$; Fig. 7b), b) Th and Ca

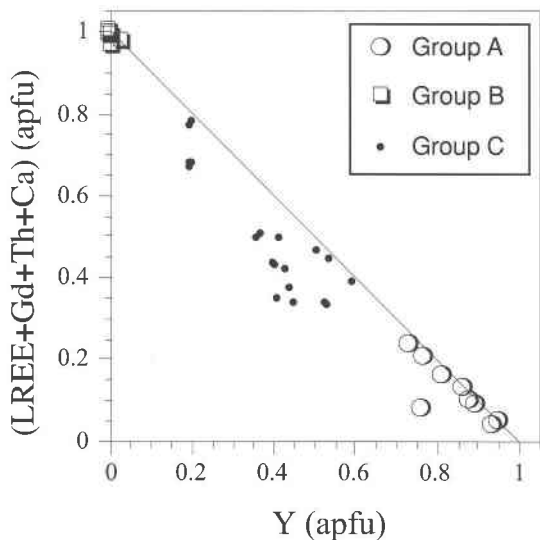


FIG. 4. Compositional variations of the analyzed *LREE*- and *Y*-arsenates in the (*LREE* + *Gd* + *Th* + *Ca*) versus *Y* binary diagram (*apfu*: atoms per formula unit).

contents generally below 0.01 *apfu* (Fig. 6), and c) low *Gd* contents (*Gd* < 0.02 *apfu*).

Group C is characterized by levels of *LREE* and *Y* intermediate between Groups A and B ($7 < Y_2O_3 < 28$ wt%; $13 < LREE_2O_3 < 34$ wt%; Table 5). The most abundant *LREE* are *Ce*, *Nd*, and *Sm* ($0.05 < Ce < 0.14$ *apfu*, $0.06 < Nd < 0.28$ *apfu*, $0.03 < Sm < 0.1$ *apfu*; Figs. 5b–d), whereas *La* and *Pr* are generally very minor constituents (Fig. 8). Moreover, *Eu* and *Gd* are significantly higher than in Group -A and -B minerals, although they vary over a wide range (Table 5). The non-*REE* elements, *Th* and *Ca*, are invariably present in significant concentrations and show a strong positive correlation (Table 5, Fig. 6). With few exceptions, *P* and *V* contents (Figs. 7a–c) are subordinate if compared to the other groups.

DISCUSSION AND CONCLUSIONS

Mineral chemistry

To date, about 150 rare-earth mineral species have been described; following the criteria suggested by Miyawaki & Nakai (1996, and references therein), the known *REE*-minerals can be classified in six main groups based on the types of anionic groups in their structure. Rare-earth minerals with structures characterized by isolated tetrahedral anionic groups are phosphates (e.g., xenotime YPO_4 and monazite $LREEPO_4$), arsenates [e.g., chernovite $YAsO_4$ and gasparite-(*Ce*), $CeAsO_4$], and vanadates [e.g., wakefieldite-(*Y*), YVO_4 and wakefieldite-(*Ce*), $CeVO_4$]. Limited solid-solutions

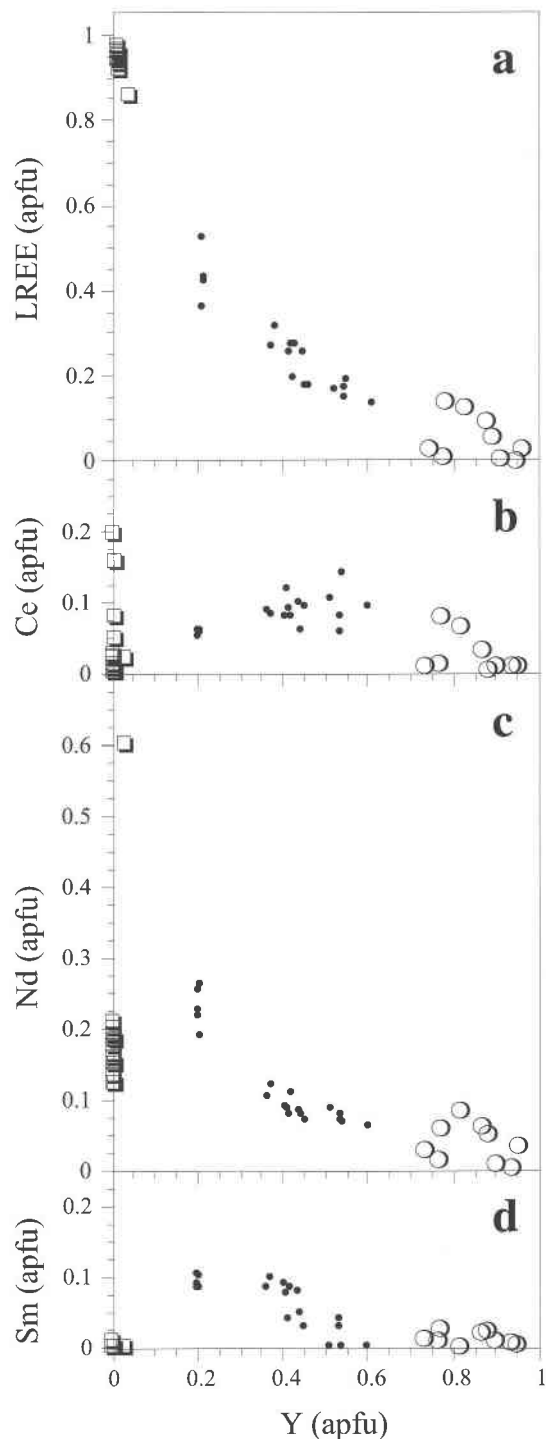


FIG. 5. Binary plots of: a) *LREE* versus *Y* contents (*apfu*), b) *Ce* versus *Y* contents (*apfu*), c) *Nd* versus *Y* contents (*apfu*), and d) *Sm* versus *Y* contents (*apfu*). Symbols and abbreviations as in Figure 4.

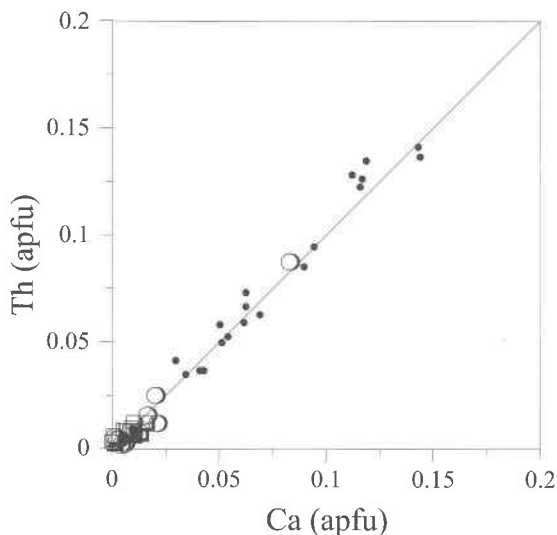


FIG. 6. Binary plot of Th versus Ca contents (apfu). Symbols and abbreviations as in Figure 4.

are known within and among these mineral groups (*e.g.*, within monazite-group minerals and between xenotime and chernovite).

In the arsenate group, only two natural phases are known: chernovite ($YAsO_4$), an isomorph of xenotime (YPO_4 ; Graeser *et al.* 1973), and gasparite-(Ce) ($CeAsO_4$), ($P2_1/n$), the arsenate analogue of monazite-Ce ($CePO_4$) (Graeser & Schwander 1987).

$LaAsO_4$ and $NdAsO_4$ are only known as synthetic compounds, and their space-group symmetry ($P2_1/n$) and cell parameters (JCPDS #15-756 and #15-643) are very similar to those of gasparite-(Ce).

The arsenates found in the Fe-Mn ores from Val Corsaglia are characterized by chemical compositions comparable to the natural and synthetic arsenates described above. Their stoichiometry fits with the structural formula ($XAsO_4$), with significant chemical variations in the three different groups of compositions (Groups A, B, and C), which could be explained by the existence of different isomorphous substitutions (Figs. 5a, 7a, and 8a).

Group-A minerals are chemically consistent with chernovite. The presence of a negative correlation between Y and LREE (Fig. 5a), enhanced if we consider Gd, Ca, and Th together with LREE (Fig. 4), suggests a limited solid-solution, up to ~30 mol% of the component ($LREE, Gd, Th, Ca$) AsO_4 . The extent of the isomorphous substitution between LREE and Y is greater than, and contrasts with, that indicated in the few known compositions of chernovite, where Y is replaced almost exclusively by HREE (Graeser *et al.* 1973). Although this is also in contrast with the crystallochemical data on xenotime, which is essentially a solid solution between YPO_4 and $HREEPO_4$ (Franz *et al.* 1996), the

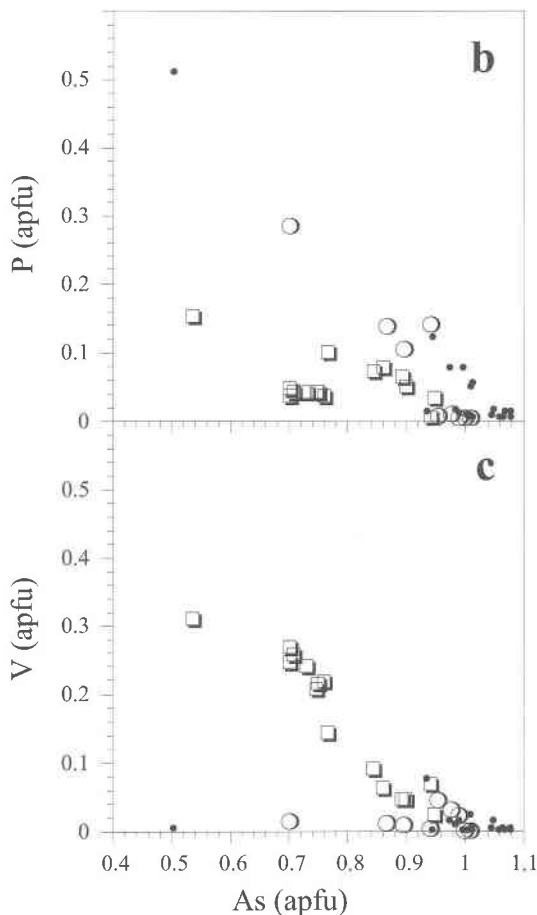
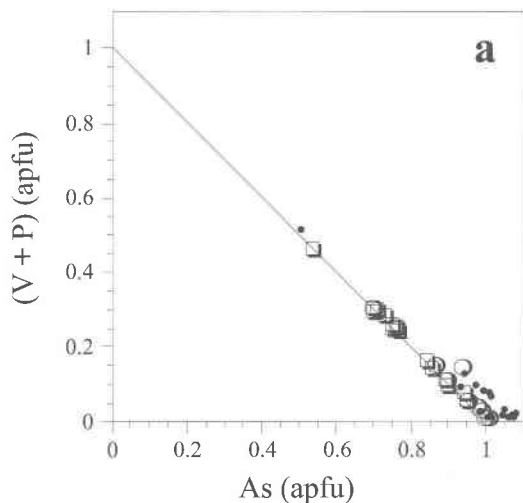


FIG. 7. Binary plots of: a) (V + P) versus As contents (apfu), b) P versus As contents (apfu), and c) V versus As contents (apfu). Symbols and abbreviations as in Figure 4.

TABLE 4. ELECTRON-MICROPROBE DATA, GRAINS OF GROUP-B ARSENATE

As ₂ O ₅ wt.%	39.51	37.55	36.11	31.87	31.95	37.44	32.60	35.49	23.45	29.86	29.93	30.24	39.83
V ₂ O ₅	0.66	1.46	1.99	6.86	7.13	1.45	4.70	2.89	10.58	8.92	8.20	8.53	2.22
P ₂ O ₅	0.75	1.17	1.94	1.02	1.02	1.55	2.49	1.76	3.98	0.86	1.15	1.00	0.03
SiO ₂	0.04	0.15	0.09	0.31	0.04	0.15	0.02	0.02	0.05	0.04	0.20	0.02	0.02
La ₂ O ₃	28.83	32.65	36.22	36.86	38.93	36.30	37.20	40.02	40.04	40.59	44.72	42.20	3.85
Ce ₂ O ₃	9.11	11.50	0.54	2.73	1.39	1.43	0.30	1.08	<0.04	<0.04	1.46	<0.04	1.09
Pr ₂ O ₃	10.76	6.44	9.80	6.22	6.92	7.91	12.57	5.78	12.85	10.33	1.71	6.05	11.27
Nd ₂ O ₃	8.97	7.43	12.20	11.26	10.84	12.66	9.81	11.48	8.36	7.50	10.07	9.35	37.05
Sm ₂ O ₃	<0.06	<0.06	<0.06	<0.06	<0.06	<0.06	<0.06	<0.06	<0.06	<0.06	<0.06	<0.06	<0.06
Eu ₂ O ₃	<0.06	0.06	<0.06	0.39	<0.06	<0.06	<0.06	<0.06	<0.06	<0.06	0.13	<0.06	0.13
Gd ₂ O ₃	0.46	0.66	0.99	0.94	1.20	0.99	<0.06	0.79	<0.06	1.07	1.14	1.28	0.47
Y ₂ O ₃	0.25	0.04	<0.04	0.17	<0.04	<0.04	<0.04	<0.04	<0.04	0.17	0.08	0.04	1.21
ThO ₂	0.38	0.48	0.10	0.98	0.39	0.10	0.29	0.58	0.60	0.58	0.98	0.49	0.88
CaO	0.20	0.18	0.02	0.35	0.23	0.04	0.04	0.12	0.17	0.14	0.23	0.29	1.78
$\Sigma LREE_2O_3$	57.67	58.08	58.76	57.46	58.08	58.30	59.88	58.36	61.25	58.42	58.09	58.05	53.39
Total	99.92	99.77	100.00	99.96	100.04	100.02	100.02	100.01	100.08	100.06	100.00	99.94	99.83
Number of ions on the basis of 4 atoms of oxygen													
As <i>apfu</i>	0.951	0.903	0.862	0.751	0.753	0.895	0.768	0.846	0.540	0.703	0.705	0.712	0.945
V	0.020	0.044	0.060	0.204	0.212	0.044	0.140	0.087	0.308	0.265	0.244	0.254	0.067
P	0.029	0.046	0.075	0.039	0.039	0.060	0.095	0.068	0.149	0.033	0.044	0.038	0.001
Si	0.002	0.007	0.004	0.014	0.002	0.007	0.001	0.001	0.002	0.002	0.009	0.001	0.001
Total	1.002	1.000	1.001	1.008	1.006	1.006	1.004	1.002	0.999	1.003	1.002	1.005	1.014
La	0.490	0.554	0.610	0.613	0.648	0.612	0.619	0.673	0.651	0.674	0.743	0.701	0.064
Ce	0.154	0.194	0.009	0.045	0.023	0.024	0.005	0.018	-	0.024	-	0.018	-
Pr	0.181	0.108	0.163	0.102	0.114	0.132	0.206	0.096	0.206	0.169	0.028	0.099	0.186
Nd	0.148	0.122	0.199	0.181	0.175	0.207	0.158	0.187	0.132	0.121	0.162	0.150	0.600
Sm	-	-	-	-	-	-	-	-	-	-	-	0.007	-
Eu	-	0.001	-	0.006	-	-	-	-	-	-	0.002	-	0.002
Gd	0.007	0.010	0.015	0.014	0.018	0.015	-	0.012	-	0.016	0.017	0.019	0.007
Y	0.006	0.001	-	0.004	-	-	-	-	-	0.004	0.002	0.001	0.029
Ca	0.010	0.009	0.001	0.017	0.011	0.002	0.002	0.006	0.008	0.007	0.011	0.014	0.087
Th	0.004	0.005	0.001	0.010	0.004	0.001	0.003	0.006	0.006	0.006	0.010	0.005	0.009
$\Sigma LREE$	0.973	0.979	0.981	0.947	0.960	0.975	0.988	0.974	0.989	0.964	0.959	0.957	0.870
Total	1.000	1.004	0.998	0.992	0.993	0.993	0.993	0.998	1.003	0.997	0.999	0.996	1.002

Analytical errors as discussed in the section on Analytical methods.

presence of the larger AsO₄ tetrahedra could enable these Y-arsenates to accept the larger *LREE* ions, as reported by Miyawaki & Nakai (1996) for the V-analogue, wakfieldite.

Group-B minerals are chemically consistent with the -(La) and, in one case, -(Nd) analogues of gasparite-(Ce); therefore, they could represent new mineral species, to date known only as synthetic compounds. Most of the analyzed phases shows a good negative correlation between La and the *other LREE* (mainly Ce, Pr and Nd), thus suggesting an isomorphous series between ~74 and ~48 mol% of LaAsO₄ (Fig. 8a). These diadochical replacements are consistent with the isomorphous substitutions described by many authors for monazite-group minerals.

Group-C phases have intermediate Y (~60–20 mol% of YAsO₄) and *LREE* (~16–56 mol% of *LREE*AsO₄) contents (Fig. 5a). Although on the basis of available data, we cannot exclude that they could represent mixtures between Groups A and B minerals, some chemical features point to the possible presence of a distinct

mineral phase. In particular, they show Th, Ca, Sm, and Gd concentrations significantly higher than Group A and B arsenates. Moreover, in most of the analyses, the sum of cations in the *REE* site is slightly lower than 1 *apfu*, thus suggesting the presence of undetected elements.

Among the three groups, the content of non-*REE* elements (Ca and Th) varies over a wide range and reaches the highest value in group-C minerals (Fig. 6); the good positive correlation between Ca and Th suggests the coupled substitution $2REE^{3+} \rightleftharpoons (Ca^{2+} + Th^{4+})$ within the *REE* site, as has been observed in many other minerals, most notably in the monazite group (Miyawaki & Nakai 1996, and references therein).

Literature data on *REE* phosphates indicate that this replacement is more common and significant in monazite than in xenotime, as a consequence of similarities in ionic radii and coordination number among *LREE* ions, Ca²⁺ and Th⁴⁺ (Miyawaki & Nakai 1996). In contrast, in the samples studied, the maximum extent of the Ca–Th coupled substitution is reached in groups A

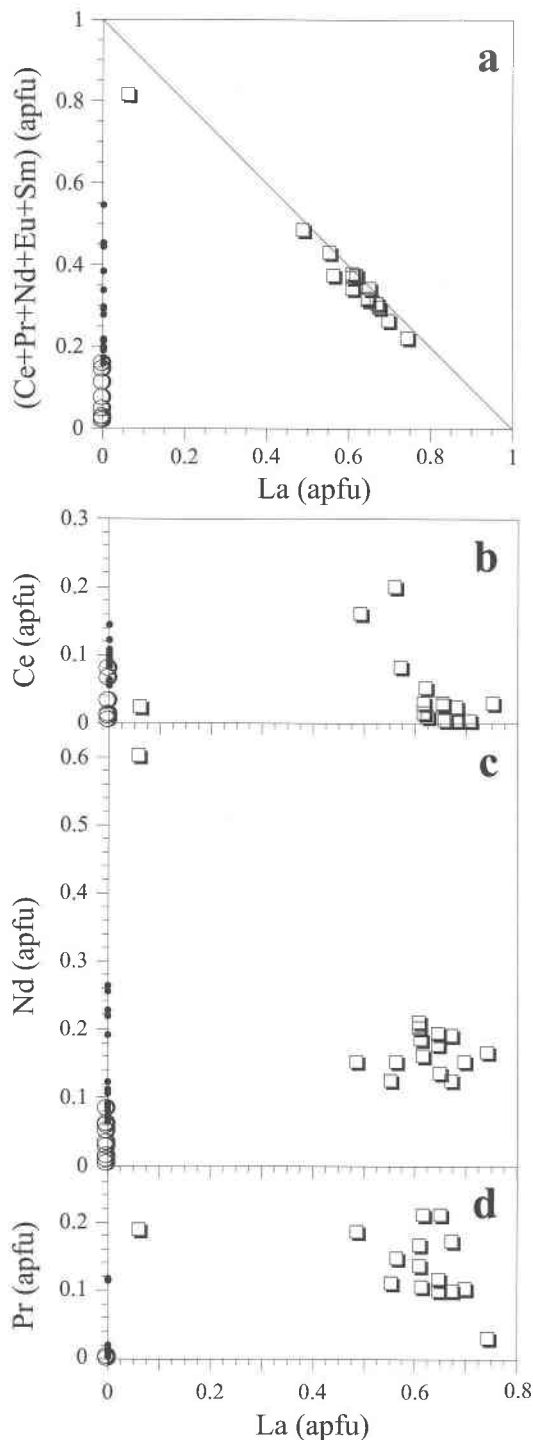


FIG. 8. Binary plots of: a) (Ce + Pr + Nd + Eu + Sm) versus La contents (apfu), b) Ce versus La contents (apfu), c) Nd versus La contents (apfu), and d) Pr versus La contents (apfu). Symbols and abbreviations as in Figure 4.

TABLE 5. ELECTRON-MICROPROBE DATA, GRAINS OF GROUP-C ARSENATE

As ₂ O ₃ wt. %	46.20	43.58	47.75	47.33	51.49	48.72	49.44	43.56	23.60
V ₂ O ₅	<0.02	2.78	0.31	0.47	0.52	0.82	0.48	<0.02	0.04
P ₂ O ₅	0.14	0.31	0.37	2.26	0.37	1.41	0.19	0.05	14.61
SiO ₂	<0.02	<0.02	2.47	0.65	1.81	1.09	4.58	0.24	0.05
La ₂ O ₃	<0.04	<0.04	<0.04	<0.04	0.07	<0.04	<0.04	<0.04	<0.04
Ce ₂ O ₃	9.11	6.71	5.39	3.75	6.31	4.03	6.33	3.48	3.57
Pr ₂ O ₃	<0.04	<0.04	0.07	<0.04	0.14	0.21	0.29	6.93	7.44
Nd ₂ O ₃	4.54	5.75	5.53	4.86	4.92	5.36	5.66	15.87	12.76
Sm ₂ O ₃	<0.06	<0.06	1.96	2.71	2.06	3.31	2.78	6.69	5.72
Eu ₂ O ₃	<0.06	<0.06	0.15	0.46	0.46	0.61	0.39	1.09	1.01
Gd ₂ O ₃	<0.06	<0.06	2.74	4.06	2.69	3.75	2.57	3.71	3.79
Y ₂ O ₃	24.20	23.14	25.19	25.17	21.59	20.82	20.11	8.17	9.12
ThO ₂	13.23	14.26	6.16	6.26	5.65	7.74	5.38	8.11	14.83
CaO	2.48	3.26	1.19	1.45	1.30	1.45	1.24	1.86	3.24
ΣLREE ₂ O ₃	13.65	12.46	13.10	11.78	13.96	13.52	15.45	34.06	30.50
Total	99.90	99.79	99.28	99.43	99.38	99.32	99.44	99.76	99.78
Number of ions on the basis of 4 atoms of oxygen									
As apfu	1.005	0.935	0.986	0.975	1.049	1.009	0.990	1.015	0.505
V	-	0.075	0.008	0.012	0.013	0.021	0.012	-	0.001
P	0.005	0.011	0.012	0.075	0.012	0.047	0.006	0.002	0.507
Si	-	-	0.098	0.026	0.071	0.043	0.175	0.011	0.002
Total	1.010	1.021	1.104	1.088	1.145	1.120	1.183	1.028	1.015
La	-	-	-	-	0.001	-	-	-	-
Ce	0.139	0.101	0.078	0.054	0.090	0.058	0.089	0.057	0.054
Pr	-	-	0.001	-	0.002	0.003	0.004	0.112	0.111
Nd	0.067	0.084	0.078	0.068	0.068	0.076	0.077	0.252	0.187
Sm	-	-	0.027	0.037	0.028	0.045	0.037	1.103	0.081
Eu	-	-	0.002	0.006	0.006	0.008	0.005	0.017	0.014
Gd	-	-	0.036	0.053	0.035	0.049	0.033	0.055	0.051
Y	0.536	0.506	0.530	0.528	0.448	0.439	0.410	0.194	0.199
Ca	0.111	0.143	0.050	0.061	0.054	0.062	0.051	0.089	0.142
Th	0.125	0.133	0.055	0.056	0.050	0.070	0.047	0.082	0.138
ΣLREE	0.206	0.185	0.186	0.165	0.195	0.191	0.212	0.541	0.446
Total	1.184	1.152	1.043	1.028	0.977	1.001	0.965	1.502	1.423

Analytical errors as discussed in the section on Analytical methods.

and C (e.g., in the Y-rich minerals); as previously discussed for the anomalously high LREE content in group-A minerals, this finding could be related to the difference in size between AsO₄ and PO₄ tetrahedra.

In groups A–C, the negative correlation between (P + V) and As (Fig. 7a) points to the existence of solid solutions involving arsenates, phosphates, and vanadates in the As-rich portion of the system. The As-for-P substitution (Fig. 7b), already observed between xenotime and chernovite (Graeser *et al.* 1973), is similar in extent among the three groups, with the highest values in Groups C and A (up to ~50 and 30 mol% of REEPO₄, respectively). Conversely, the As-for-V substitution (Fig. 7c) take place almost exclusively in group B (up to ~30 mol% of LREEVO₄), suggesting a solid solution with wakefieldite.

Genetic hypothesis

REE arsenates are invariably present within the mineralized layers and lenses hosted in quartz arenites and, to a lesser extent, in marbles of the Val Corsaglia sequence. Their mode of occurrence suggests that they

precipitated from solutions circulating in an open space, mainly represented by microveins and irregular microcavities.

Considering the data on whole-rock chemistry and the relative low mobility of *REE*, it can be inferred that the elements necessary for the growth of *REE*-arsenates were mobilized from the adjacent Fe- and Mn-mineralized layers and partitioned in the circulating fluids. Enrichments in heavy metals, *REE*, Y, As, and Th have been described by many authors (Roy 1981, and references therein; Kunzendorf *et al.* 1993, Glasby *et al.* 1997) from Fe–Mn ores of various modes of formation, where they are generally incorporated into the primary ore-minerals. Moreover, the mobilization of *REE* and As from a Fe–Mn deposit by circulating fluids under lower greenschist-facies conditions has been recently documented (Brugger & Gieré 1999).

We cannot be definitive about the processes through which these elements were mobilized and transported during vein formation because, to date, it has not been possible to perform systematic studies on fluid chemistry (*i.e.*, fluid-inclusion studies). Nevertheless experimental data and geochemical evidence reported in the literature on a wide range of geological settings (Haas *et al.* 1995, and references therein) suggest that the *REE* could be mobilized and transported in aqueous solutions mainly as complexes (*e.g.*, *REE* hydroxide, chloride, and fluoride) rather than as unassociated ions.

The precipitation of *REE* arsenates presumably occurred as a consequence of a residual enrichment of *REE* and As in the circulating fluids, since these elements are not significantly incorporated in the other vein-filling minerals (*e.g.*, quartz, phengitic mica).

The timing of these events is well constrained by textural evidence. In fact, arsenate-bearing minerals mainly occur in microveins that cross-cut the metamorphic assemblage or line the crystal boundaries of the granoblastic braunite + quartz ore assemblage. This evidence indicates that their genesis must have occurred after the peak of metamorphism (blueschist-facies conditions; $P \geq 7$ kbars; $T = 300^\circ \pm 50^\circ\text{C}$), during an episode of brittle deformation that accompanied the decompression and retrograde adjustments.

ACKNOWLEDGEMENTS

This study was supported by the MURST project "Relations between structure and properties in minerals: analysis and applications". The electron-microprobe work at the Dipartimento di Scienze della Terra, University of Modena, was made possible by financial support of the CNR of Italy. We are grateful to G. Garuti for useful discussions. The authors thank R. Gieré, S. Graeser, and R.F. Martin for their careful reviews.

REFERENCES

- BRUGGER, J. & GIERÉ, R. (1999): As, Sb, Be and Ce enrichment in minerals from a metamorphosed Fe–Mn deposit, Val Ferrera, eastern Swiss Alps. *Can. Mineral.* **37**, 37–52.
- CABELLA, R., GAGGERO, L. & LUCCHETTI, G. (1992): Hollandite–cryptomelane and braunite in Mn-ores from upper Jurassic meta-arenites and marbles (Internal Briançonnais, Maritime Alps). *Rend. Fis. Acc. Lincei, Ser. 9*, **3**, 33–41.
- _____, LUCCHETTI, G. & MARESCOTTI, P. (1995): Sr-rich hollandite and cryptomelane in braunite-ores of Maritime Alps and eastern Liguria (Italy). *Neues Jahrb. Mineral. Monatsh.*, 395–407.
- CHANG, L.L.Y., HOWIE, R.A. & ZUSSMAN, J. (1996): *Rock-Forming Minerals. 5B. Non-Silicates: Sulfates, Carbonates, Phosphates and Halides*. Longman, London, U.K.
- DALLAGIOVANNA, G. (1993): Considerazioni stratigrafiche sulle successioni piemontesi e brianzonesi affioranti nel Monregalese e sul loro ruolo paleogeografico durante il Mesozoico. *Atti Tic. Sci. Terra* **36**, 51–73.
- DONOVAN, J.J. & RIVERS, M.L. (1990): A PC based automation and analysis software package for wavelength-dispersive electron-beam microanalysis. *Microbeam Analysis* **25**, 66–68.
- DRAKE, M.J. & WEILL, D.F. (1972): New rare earth element standards for electron microprobe analysis. *Chem. Geol.* **10**, 179–181.
- FRANZ, G., ANDREHS, G. & RHEDE, D. (1996): Crystal chemistry of monazite and xenotime from Saxothuringian–Moldanubian metapelites, NE Bavaria, Germany. *Eur. J. Mineral.* **8**, 1097–1118.
- GIERÉ, R. (1996): Formation of rare earth minerals in hydrothermal systems. In *Rare Earth Minerals. Chemistry, Origin and Ore Deposits* (A.P. Jones, F. Wall & C.T. Williams, eds.). Chapman & Hall, London, U.K. (105–150).
- GLASBY, G.P., STÜBEN, D., JESCHKE, G., STOFFERS, P. & GARBE-SCHÖNBERG, C.-D. (1997): A model for the formation of hydrothermal manganese crusts, from the Pitcairn Island hotspot. *Geochim. Cosmochim. Acta* **61**, 4583–4597.
- GRAESER, S. & SCHWANDER, H. (1987): Gasparite-(Ce) and monazite-(Nd): two new minerals to the monazite group from the Alps. *Schweiz. Mineral. Petrogr. Mitt.* **67**, 103–113.
- _____, _____ & STALDER, H.A. (1973): A solid solution series between xenotime (YtPO₄) and chernovite (YtAsO₄). *Mineral. Mag.* **39**, 145–151.
- HAAS, J.R., SHOCK, E.L. & SASSANI D.C. (1995): Rare earth elements in hydrothermal systems: estimates of standard partial molal thermodynamic properties of aqueous complexes of the rare earth elements at high pressures and temperatures. *Geochim. Cosmochim. Acta* **59**, 4329–4350.

- KUNZENDORF, H., GLASBY, G.P., STOFFERS, P. & PLÜGER, W.L. (1993): The distribution of rare earth and minor elements in manganese nodules, micronodules and sediments along an east-west transect in the Southern Pacific. *Lithos* **30**, 45-56.
- MIYAWAKI, R. & NAKAI, I. (1996): Crystal chemical aspects of rare earth minerals. *In* Rare Earth Minerals. Chemistry, Origin and Ore Deposits (A.P. Jones, F. Wall & C.T. Williams, eds.). Chapman & Hall, London, U.K. (21-40).
- ROY, S. (1981): *Manganese Deposits*. Academic Press, London, U.K.
- _____ (1992): Environments and processes of manganese deposition. *Econ. Geol.* **87**, 1218-1236.
- VANOSI, M., CORTESOGNO, L., GALBIATI, B., MESSIGA, B., PICCARDO, G.B. & VANNUCCI, R. (1986): Geologia delle Alpi Liguri: dati, problemi e ipotesi. *Mem. Soc. Geol. It.* **28**, 5-75.
- WYLLIE, P.J., JONES, A.P. & DENG, J. (1996): Rare earth elements in carbonate-rich melts from mantle to crust. *In* Rare Earth Minerals, Chemistry, Origin and Ore Deposits (A.P. Jones, F. Wall & C.T. Williams, eds.). Chapman & Hall, London, U.K. (77-103).
- WU, C., YUAN, Z. & BAI, G. (1996): Rare earth deposits in China. *In* Rare Earth Minerals, Chemistry, Origin and Ore Deposits (A.P. Jones, F. Wall & C.T. Williams, eds.). Chapman & Hall, London, U.K. (281-310).

Received February 23, 1999, revised manuscript accepted July 27, 1999.